highly deformed terrain are mapped as tesserae. Unlike Beta Regio, tesserae does not appear to be a major unit Atla [9].

Ozza Mons forms the central part of Atla and is located at the point where Ganis, Dali, and Parga Chasma intersect. The relationship between Ganis Chasma and Ozza Mons is examined along with the general stratigraphic relationships between assemblages of volcanic units. The rift valley, Ganis Chasma, is unique in that it is relatively devoid of infilling from volcanism and sedimentary material. The exception to this trend is evident where it merges with the volcano. At the point where the rift intersects Ozza it narrows from a width of 225 km to 125 km and deformation is confined to a trough on the flank of the volcano. The primary area of disruption is a zone of scarps associated with normal faulting that is offset from the main trend of the rift, changing orientation from a strike that is just west of north to one that is just east of north. Additional scarps with a relatively uniform spacing of 5 km are arrayed with a northeast/southwest orientation on the eastern flank of the edifice and are associated with an unnamed rift aligned to the northeast. The Ganis rift terminates at the summit of Ozza, a radar-dark oval plateau (100 km × 60 km) that rises to an elevation of 1.5 km above its surroundings and contains numerous pits and collapse structures (diameters of 0.5 to 7.0 km). To the north of the summit, just below the plateau, lies a dome field (domes 10 km in diameter) covering an area 80 km × 100 km. Deposits along the eastern edge of the dome field are superposed on faults and fractures from Ganis Chasma, indicating that at this location volcanism postdates faulting and contributes to partial infilling of the rift. Further to the north, where the rift narrows, other lava flows both superpose and are cross cut by faults, indicating that rifting and the deposition of volcanics occurred concurrently.

Four major classes of volcanic deposits are identified on Ozza Mons; the first two are made up of the radar-dark material on the summit and the adjacent dome field. The others correspond to flow units mapped on the distal parts of the volcano, bright flows and mottled bright flows. Bright flows have a relatively uniform texture, with no apparent source regions for the deposits observed. In many places the unit is cut by faults and fractures, deformation associated with rifting. In comparison, it is possible to identify numerous apparent source regions for mottled bright flows. These originate mainly from vents on the outer flanks of the volcano. Like the bright flow unit it is possible to identify places where the mottled bright flows are cross cut by faulting. The boundaries between the units typically form an embayment relationship, with some of the mottled bright flows being channeled down graben, suggesting that they are stratigraphically the younger of the two units. In general the dome field and the mottled bright flows appear to be most recent units.

Maat Mons: Located 600 km southwest of Ozza Mons and lying on the northwest edge of Dali Chasma is Maat Mons. In plan view, this volcano is elliptically shaped (195 km × 120 km) with its major axis oriented in a northeast/southwest direction. Its summit region differs from that of Ozza Mons in that it contains a 25-km-diameter caldera with additional smaller nested pits and collapse structures (diameters between 1.0 and 5.0 km), indicating multiple episodes of magma emplacement and withdrawal. Unlike Ozza Mons, this volcano is not disrupted by faulting, but instead, along its southeast flank, appears to be filling the rift.

Volcanic deposits mapped on Maat range from bright to mottled dark. The most abundant flows have a bright homogeneous texture, are found on the more distal flanks of the volcano, and are interpreted to be associated with the large-scale effusion of lava. Mottled bright flows have a range of textures on the scale of tens of kilometers and are found mainly in the area where the rift is being filled in. The central part of Maat contains deposits with mottled dark textures that are arrayed in a pattern radial to the summit. In several locations the dark material has a diffuse boundary, suggesting the presence of a mantling deposit. One example corresponds to a cluster of domes (diameters ranging from 5 to 10 km) located in a 2.0 km deep depression 250 km to the north of the summit (3.2°N, 194.9°) and mapped as a dome field. The terrain associated with this area appears etched and is covered by a dark diffuse deposit, suggesting the possible presence of an air fall deposit associated with pyroclastic activity. In general the boundaries between the different flow units are gradational, making stratigraphic relationships difficult to determine.

Summary and Conclusions: Atla Regio is a complex region of converging rifts and volcanism. The largest (areally extensive) volcanic center corresponds to Ozza Mons and has characteristics similar to Theia Mons in Beta Regio [5]. Stratigraphic relationships at Ozza suggest that both the deposition of volcanics and rifting have occurred concurrently. Maat Mons is broadly similar to volcanos identified in Western Eistla Regio (Sif Mons) and contains a well-defined summit caldera. On the basis of regional stratigraphic relationships and the analysis of geophysical data, Atla is interpreted to be a site in which a mantle plume, centered near Ozza Mons, has uplifted plains causing faulting and rifting and volcanic construction at Ozza Mons and Maat Mons.

In addition to Ozza Mons, Sapas Mons, Ganis Chasma, and the area mapped as a volcanic center (separate from the large volcanos), all have substantial positive gravity anomalies. Sapas is interpreted to be a second site of upwelling adjacent to Atla. On the basis of its large gravity anomaly and a corresponding large apparent depth of compensation (>200 km) [7] the zone of extension and rifting at Ganis is interpreted to be linked to mantle dynamics. This array of surface features separate from those at central Atla (Ozza and Maat) may be associated with multiple upwellings, or possibly a single large plume that has produced smaller instabilities [10].

References: [1] Senske D. A. (1990) *Earth Moon Planets, 50/51*, 305–327. [2] Senske D. A. et al. (1991a) *Earth Moon Planets, 55*, 163–214. [3] Campbell D. B. et al. (1984) *Science, 226*, 167–170. [4] Stofan E. R. et al. (1989) *GSA Bull., 101*, 143–156. [5] Senske D. A. et al. (1992) *JGR, 97*. [6] Sjogren W. L. et al. (1983) *JGR, 88*, 1119–1128. [7] Smrekar S. E. and Phillips R. J. (1991) *EPSL, 107*, 582–597. [8] Sjogren et al. (1983) *JGR, 88*, 1119–1128. [9] Senske D. A. et al. (1991b) *GRL, 18*, 1159–1162. [10] Griffiths R. W. and Campbell I. H. (1991) *JGR, 96*, 18295–18310.

N93-14375

THE GEOLOGIC MAPPING OF VENUS USING C-1 FORMAT: SHEETS 75N254, 60N263.

I. V. Shalimov, Lomonosov Moscow University, Moscow, Russia

The results of geologic mapping of Venus, produced on the base of Magellan images, are presented. We submit two C-1 format geologic maps with the appropriate legend.

The mapping territory has been taken from Venera 15 and 16 missions and geologic maps have been composed by Sukhanov et al. [2] and Kotelnicov et al. [1]. Magellan images allow us to divide some types of the plains units to determine the lava flow direction and to map with better accuracy.

C-1 sheets 75N254 and 60N263 are shown in Figs. 1 and 2. The correlation of the mapped units is shown in Fig. 3. We regret the difficult perception without the color legend.

References: [1] Kotelnicov V.A. et al. (1989) *Atlas of Venus*, GUGK, Moscow (in Russian). [2] Sukhanov A.L. et al. (1989) *Atlas*

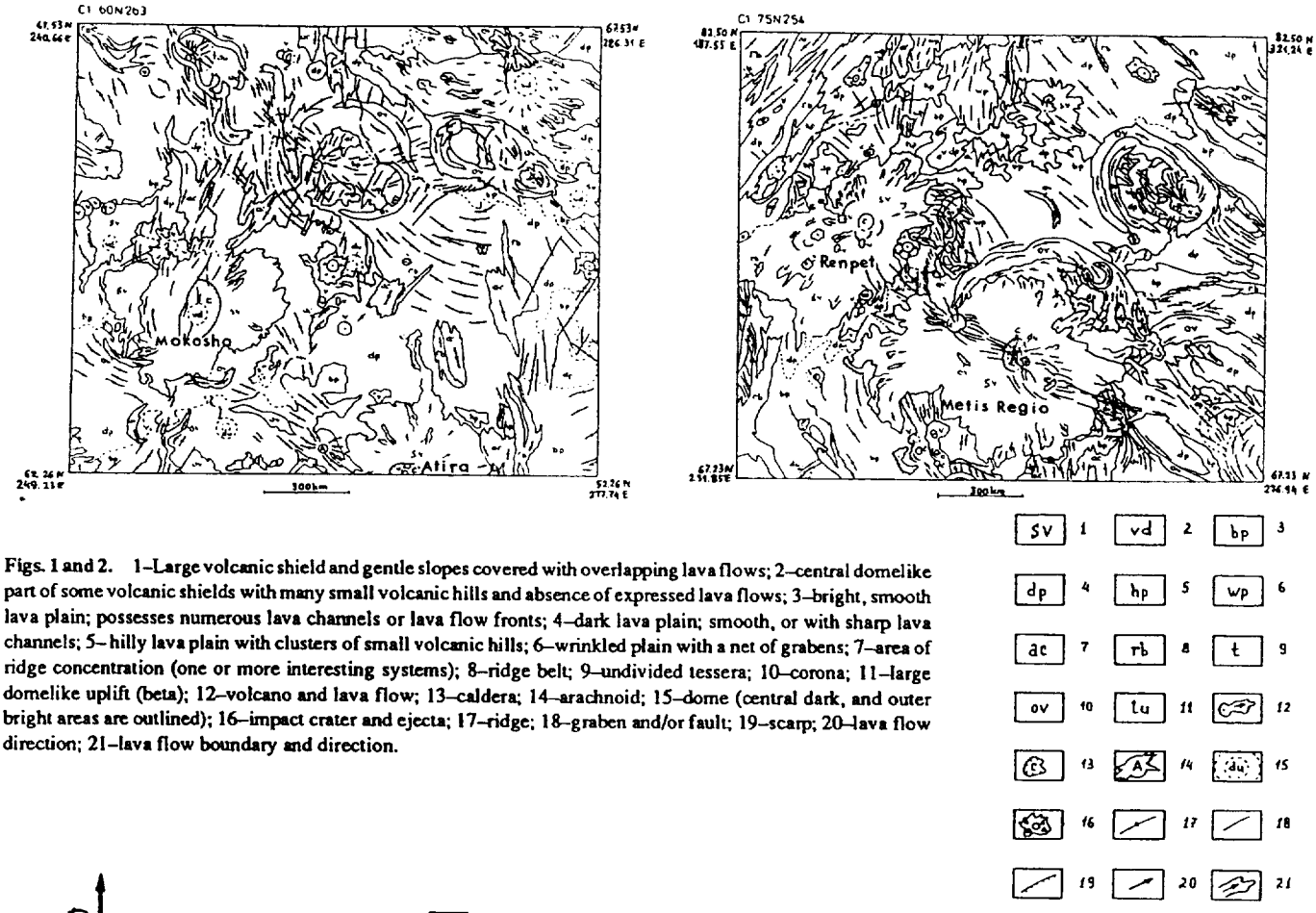

Figs. 1 and 2. 1–Large volcanic shield and gentle slopes covered with overlapping lava flows; 2–central domelike part of some volcanic shields with many small volcanic hills and absence of expressed lava flows; 3–bright, smooth lava plain; possesses numerous lava channels or lava flow fronts; 4–dark lava plain; smooth, or with sharp lava channels; 5–hilly lava plain with clusters of small volcanic hills; 6–wrinkled plain with a net of grabens; 7–area of ridge concentration (one or more interesting systems); 8–ridge belt; 9–undivided tessera; 10–corona; 11–large domelike uplift (beta); 12–volcano and lava flow; 13–caldera; 14–arachnoid; 15–dome (central dark, and outer bright areas are outlined); 16–impact crater and ejecta; 17–ridge; 18–graben and/or fault; 19–scarp; 20–lava flow direction; 21–lava flow boundary and direction.

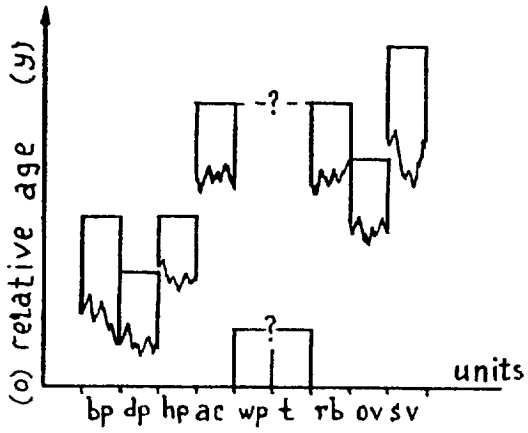

Fig. 3. Correlation of the mapped units shown in Figs. 1 and 2.

of Venus, 1:15,000,000 topographic series, northern hemisphere, V. 15M 90/G, I–2059. U.S. Geol. Surv.

N93-14376

GEOID, TOPOGRAPHY, AND CONVECTION-DRIVEN CRUSTAL DEFORMATION ON VENUS. Mark Simons, Bradford H. Hager, and Sean C. Solomon, Department of Earth, Atmospheric, and Planetary Sciences, Massachusetts Institute of Technology, Cambridge MA 02139, USA.

Introduction: High-resolution Magellan images and altimetry of Venus reveal a wide range of styles and scales of surface deformation [1] that cannot readily be explained within the classical terrestrial plate tectonic paradigm. The high correlation of long-wavelength topography and gravity and the large apparent depths of compensation suggest that Venus lacks an upper-mantle low-viscosity zone [2–5]. A key difference between Earth and Venus may be the degree of coupling between the convecting mantle and the overlying lithosphere. Mantle flow should then have recognizable signatures in the relationships between surface topography, crustal deformation, and the observed gravity field [6,7].

Model: We explore the effects of this coupling by means of a finite element modeling technique. The crust and mantle in these models are treated as viscous fluids. We solve both the equations of motion and the heat equation at every time step using a modified version of the two-dimensional Cartesian finite-element program ConMan [8]. A passive marker chain tracks the crust-mantle interface and permits variation in the crustal buoyancy as well as specific crustal and mantle rheologies. These rheologies depend on composition, temperature, and stress. In addition to the flow field, the stress field in the lithosphere, the surface topography, and the resulting geoid are readily calculated. The models presented here use an irregular finite-element mesh that is 50 elements high and 160 elements wide. Our maximum resolution is in the 40-km-thick top layer, where each element is 2 km high and 5 km wide. In all, the mesh is 800 km in the horizontal dimension and 400 km in the vertical dimension. We impose free-slip boundary conditions on the top and side walls, with no flow through these walls. Flow at the bottom boundary is constrained to be vertical with no horizontal flow permitted. This last boundary condition gives a virtual 800 km × 800 km box. The surface topography is calculated from the vertical stresses on the top wall of the box. Top and bottom